Biosensors and Bioelectronics 136 (2019) 76–83

Contents lists available at ScienceDirect

Biosensors and Bioelectronics

journal homepage: www.elsevier.com/locate/bios

384-Channel electrochemical sensor array chips based on hybridization-triggered switching for simultaneous oligonucleotide detection

Hiroshi Aoki*, Masaki Torimura, Tetsuya Nakazato

National Institute of Advanced Industrial Science and Technology (AIST), 16-1 Onogawa, Tsukuba, Ibaraki, 305-8569, Japan

ARTICLE INFO

Keywords:
DNA
RNA
Non-labeling detection
Sensor array
Environmental and biomedical diagnoses

ABSTRACT

We investigated the feasibility of simultaneous detection of multiple environmentally- and biomedically-relevant RNA biomarker target sequences on a single newly fabricated 384-ch sensor array chip aiming at practical application. The individual sensor is composed of a photolithographically-fabricated Au/Cr-based electrode modified with peptide nucleic acid (PNA) probes. The sensor array chips showed sequence-specific responses upon hybridization of the probes with target sequences complementary to the probes in contrast to mismatch versions. The target oligonucleotides have 15–22 mer sequences from messenger RNAs for estrogen-responsive genes and microRNAs for lung cancer biomarkers. The dependence on target concentrations of sensor responses was observed by using a single chip on which experiments for detection of several target concentrations proceeded simultaneously, with the detection limit of 7.33×10^{-8} M. As more realistic samples, oligonucleotide samples amplified by PCR from a synthesized template sequence were applied to the chip. They showed sequence-specific responses, revealing the potential for fabricated sensor array chips to be utilized to analyze PCR samples. Unlike complicated and expensive chips that require nanofabrication, our sensor array chips based on glass coated with gold thin films are simple and can be fabricated from inexpensive and readily available materials.

1. Introduction

The American Chemical Society's CAS Registry, the largest database of chemical substances in the world, has registered more than 140 million kinds of synthetic chemical substances (August 2018, CAS Registry, 2018). To be able to utilize these chemicals safely and effectively, it is important to evaluate and understand their biomedical effects on human health and their biological effects on ecosystems. We need to evaluate the effects of these chemicals not only individually but also in combination. This is because they are present in the environment in the form of mixtures with other chemicals, alongside their derivatives, as impurities, metabolites produced in biological systems, and degraded products.

Cell-based bioassays are increasingly widely utilized as an alternative to animal testing, both for ethical reasons and for their advantage of rapidity(Alexander-Dann et al., 2018; Borlak, 2005; Huang, 2013; Wagner and Plewa, 2017). Assays are usually performed using oligonucleotide detection techniques that include polymerase chain reaction (PCR) methods and DNA microarray procedures based on the fluorescence labeling of target DNAs and RNAs, representing biological responses to external stimuli. With the range chemicals that need to be evaluated continuing to expand, there is a growing need for evaluation of chemicals in the environment by in-situ fast screening(Campana and Wlodkowic, 2018). Rapid, simple and cost-effective screening techniques are therefore needed as an improvement to the conventional techniques used to detect oligonucleotides.

These oligonucleotide detection techniques that use DNA and RNA as indicators can also be employed for biomedical diagnoses. Cancer diagnosis is potentially one of these applications. In the past decade, it has become increasingly apparent that micro RNAs (miRNAs) are present in the blood of cancer patients and that they are specific to the types and stages of the cancers in question(Bonci et al., 2016; Kim et al., 2015; Kreth et al., 2018; Wang et al., 2016). Moreover, miRNAs are considered to be the first biomarkers to respond to changes in physical condition, making them ideal for use in preemptive medicine. Detection and identification of such miRNAs as disease biomarkers might contribute to disease prevention at an early stage. Feasible and first aid screening techniques are promising as medical diagnostic tools.

To achieve faster and simpler screening techniques, many researchers have developed oligonucleotide detection techniques based on a variety of approaches, including optical, microgravimetric, and electrochemical techniques(Sassolas et al., 2008). Electrochemical

* Corresponding author.
E-mail address: aoki-h@aist.go.jp (H. Aoki).

https://doi.org/10.1016/j.bios.2019.04.047
Received 22 February 2019; Received in revised form 22 April 2019; Accepted 23 April 2019
Available online 25 April 2019
0956-5663/

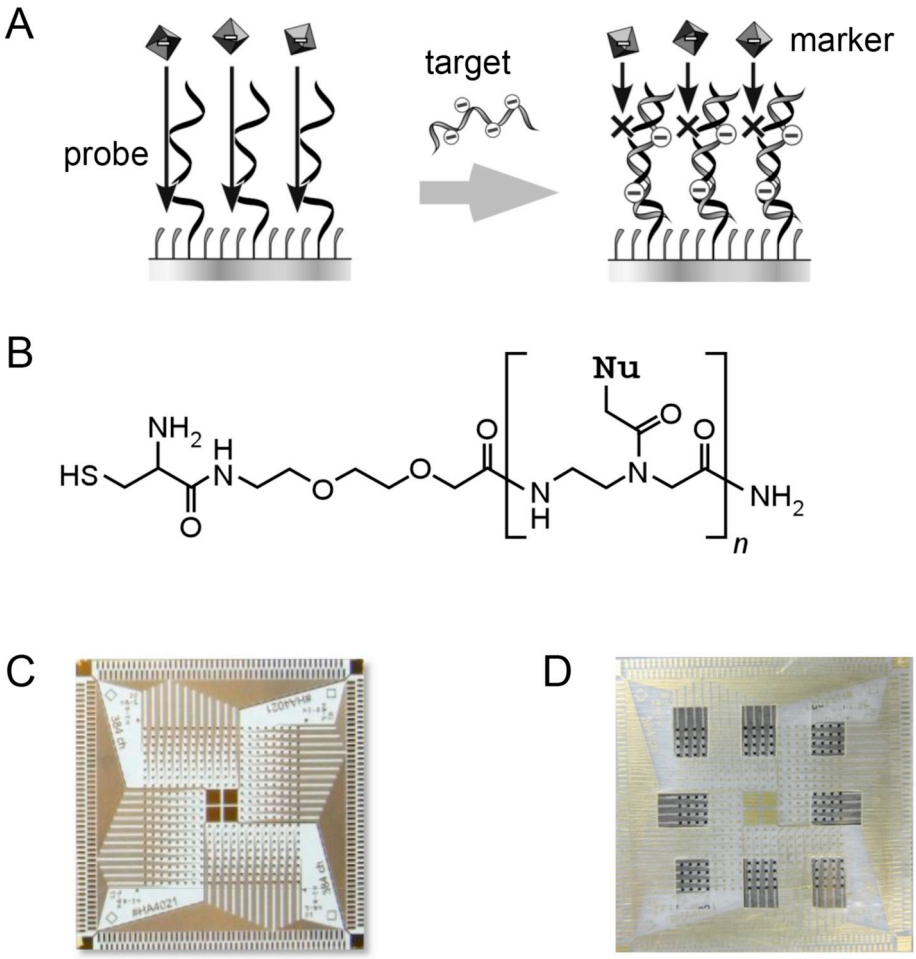

Fig. 1. Oligonucleotide detection method based on switching controlled by hybridization-amenable accumulation of charge (A) and chemical structure of probe PNA (B). Photolithographically fabricated 384-ch microelectrode array chip (C) and hydrophobic adhesive film with eight open windows for 4 × 4 electrode array blocks (D).

techniques have significant advantages because of their simple design, inherently small dimensions, and low power requirements, contributing to simpler and more compact oligonucleotide detection systems(Aoki, 2015; Bard and Faulkner, 2001; Lucarelli et al., 2008; Paleček and Bartošík, 2012; Sadik et al., 2009; Teles and Fonseca, 2008; Wang, 2005, 2006). Aiming at feasible fast screening both in the natural environment and at clinics, we have studied electrochemical oligonucleotide detection techniques based on hybridization-triggered "on/off" switching architecture without the need to label target oligonucleotides (Aoki, 2012, 2015). One of our detection techniques is based on electrostatic switching of the redox reaction of a charged redox marker (e.g., $[Fe(CN)_6]^{4-}$), controlled by hybridization-amenable accumulation of negative charge in the target oligonucleotides on the sensor surface, based on peptide nucleic acid (PNA) probes (Fig. 1A). Previous detailed reports have revealed the sensors to identify the target oligonucleotides sequence-specifically and with detection limits at the 10^{-11} M(Aoki, 2012; Aoki and Tao, 2005) level. These detection limits correspond to 10^{-15} mol (1 fmol) in 100 μL of solution. This sensor method matches the performance of conventional fluorescence labeling-based methods, with the additional advantage of no labeling step(Fiammengo, 2017).

In this study, employing the above method, we demonstrated simultaneous detection of multiple oligonucleotide biomarker sequences on a single newly fabricated 384-channel sensor array chip for more comprehensive and practical usages. Previously, we demonstrated preliminary oligonucleotide detection based on 9-ch and 96-ch addressable sensor array chips(Aoki et al., 2010a, b), in which these chips were evaluated by using only one target oligonucleotide sequence for one chip. The present sensor array chip was prepared from a photolithographically fabricated Au/Cr-based microelectrode array chip modified with several probe PNAs with sequences complementary to the targets. As the sequences of the targets, we used RNA biomarker sequences from messenger RNAs (mRNAs) for estrogen-responsive genes and microRNAs (miRNAs) for lung cancer biomarkers. Hybridization of the targets with the corresponding probes on the chip showed sequence-specific sensor responses with the detection limit of 7.33×10^{-8} M. For mismatched oligonucleotides, however, the sensors showed only small responses. As more realistic samples, oligonucleotide samples with target sequences amplified by PCR from a synthesized template sequence were applied to the sensor array chips. These showed sequence-specific responses, revealing that the fabricated sensor array chips could be utilized for PCR samples after standard purification.

2. Materials and methods

2.1. Reagents

The sequences used in this study were from the National Center for Biotechnology Information (NCBI)(National Center for Biotechnology Information, 2018). Purchased from Eurofins Genomics Japan (Tokyo, Japan) were oligonucleotides with the sequences listed in Table 1. The artificially synthesized oligonucleotide probes listed in Table 1, purchased from CBC (Tokyo, Japan), were designed as conjugates of peptide nucleic acids (PNAs) and other moieties, where O and Cys denote

Table 1
Sequences of the probe PNAs and target DNAs used in this study.

	Sequences	Name	NCBI Accession #	Remarks
Target DNAs	5′ AGA CAG CAA TAA CCA CAG TA 3′	DNA_1	L27560	Insulin-like growth factor binding protein 5 (IGFBP5)
	5′ GTG GAG TAA TAG GGA AGG TTG C 3′	DNA_2	X63741	Early growth receptor 3 (EGR3)
	5′ CGT GAA AGA CAG AAT 3′	DNA_3	XM_009779	Trefoil factor family 1 (TFF1)
	5′ ACT GCA GTG AAG GCA CTT GT 3′	DNA_4	hsa-miR-17	Lung cancer biomarker
	5′ TAG CTT ATC AGA CTG ATG TT 3′	DNA_5	hsa-miR-21	Lung cancer biomarker
	5′ GGG TAT TTG ACA AAC TGA CA 3′	DNA_6	hsa-miR-223	Lung cancer biomarker
Probe PNAs	TAC TGT GGT TAT TGC TGT CT-O-Cys-NH_2	PNA_1		Complementary to DNA_1
	ACA AGT GCC TTC ACT GCA GT-O-Cys-NH_2	PNA_4		Complementary to DNA_4
	AAC ATC AGT CTG ATA AGC TA-O-Cys-NH_2	PNA_5		Complementary to DNA_5
	GGG TAT TTG ACA AAC TGA CA-O-Cys-NH_2	PNA_6		Complementary to DNA_6
Template	5′ TGT TGT TTT TCT TTT TCT TTT TTT TTT TGA AGA CAG CAA TAA CCA CAG TAC ATA TTA CTG TAG TTC TCT ATA GTT TTA CAT ACA TTC ATA CCA TAA CTC T 3′	Template	L27560	The underlined part is recognized by PNA_1
Primers	5′ TAG AGA ACT ACA GTA ATA TG 3′	PCR_11		
	5′ AAA AAA AAG AAA AAG AAA AAC AAC A 3′	PCR_12		
	5′ AGA GTT ATG GTA TGA ATG TAT 3′	PCR_21		
	5′ TAC TGT GGT TAT TGC TGT CT 3′	PCR_22		

an ethylene glycol unit and a cysteine group, respectively (Fig. 1B). In the study of PCR products, PNA_1 was used as a probe PNA from CBC, and a template and primers were from Eurofins Genomics. 6-Hydroxy-1-hexanethiol (6-HHT) was from Dojindo (Kumamoto, Japan). All aqueous solutions were prepared with deionized and charcoal-treated water (specified resistance > 18.2 MΩ cm), obtained using a Milli-Q reagent grade water system (Millipore; Bedford, MA).

2.2. Preparation of sensor array chips

A 384-ch microelectrode array chip (384 channels; array interval, 1 mm; diameter, 300 μm) was photolithographically fabricated in a manner similar to that reported in our previous papers (Aoki et al., 2010a, b) or fabricated by NTT advanced technologies in the same manner as ours, briefly described in Supplementary Information. The fabricated 384-ch electrode array chip is shown in Fig. 1C.

A sensor array chip was prepared by modifying the electrode surfaces of the fabricated microelectrode array chip with probe PNAs and 6-HHT as follows. One-μL aliquots of a solution of 1:1100 μM probe PNAs in 0.1% trifluoroacetic acid (TFA) aqueous solution–50% glycerol aqueous solution were dispensed onto the electrode surfaces. After 30 min of immersion, the array chip was rinsed with a 0.1% TFA aqueous solution and water, and dried by N_2 blow. A 200-μL aliquot of 1 mM 6-HHT aqueous solution was then dropped on the chip to cover all the electrodes. After 30 min immersion, the array chip was rinsed with water and subjected to electrochemical measurements. The surface density of probe PNAs were estimated by using a ferrocene-modified probe PNA, briefly described in Supplementary Information. The density was induced to be $(9.03 \pm 4.23) \times 10^{-11}$ mol cm^{-2} ($n = 7$). In this modification process, electrode areas were separated from each other by placing adhesive films as hydrophobic boundaries on the chip so as to soak different electrodes in solutions containing different probe PNAs (shown in Fig. 1D). The films were prepared from Parafilm (Bemis; Oshkosh, WI) by cutting with a CC330-20 cutting plotter (Graphtec; Kanagawa, Japan).

2.3. Preparation of PCR-amplified oligonucleotide samples

To demonstrate the detection of PCR products, PCR-amplified oligonucleotide samples were prepared by basically following the protocol for Pyrobest DNA polymerase (Takara Bio; Shiga, Japan), briefly described in Supplementary Information(Takara Bio, 2018). This process produced 70-mer PCR_1 and PCR_2 oligonucleotides as predominant PCR products. These PCR products were then purified by following the protocol for Wizard SV Gel and PCR Clean-up System (Promega; Madison, WI), briefly described in Supplementary Information(Promega, 2018). The concentrations of the PCR products were measured using a NanoDrop 2000 (Thermo-Fisher, Tokyo, Japan) to prepare solutions containing 150 nM of PCR products.

2.4. Electrochemical measurements

Electrochemical measurements of the sensor array chips were performed in a 5 mM $NaClO_4$ + 2.5 mM phosphate buffer solution (pH 7.0, Na^+ salt) containing 1 mM $K_4[Fe(CN)_6]$ as the electroactive marker at 25 °C before and after incubation in an aqueous solution containing DNAs. A three-electrode configuration was used, consisting of the prepared sensor as the working electrode, an Ag/AgCl reference electrode (internal solution: 3 M NaCl), and a platinum auxiliary electrode. The electrochemical measurements were performed using the same system as previously reported(Aoki et al., 2010a).

The electrochemical cell was constructed by placing a silicone rubber frame (size, 28 mm × 28 mm; thickness, 3 mm; frame width, 3 mm) on the prepared sensor array chip filled with 1 mL of the measurement solution, with the reference and auxiliary electrodes inserted into the solution perpendicularly and close to the chip. For cyclic voltammograms (CVs), the potential was scanned from 0 to +0.5 V and again back to 0 V at a scan rate of 0.1 V s^{-1}. The sensor response to the DNAs was expressed as the ratio of peak current (i) to the current decrease ($i_0 - i$) at the peak potential (E_p) in the voltammograms measured before incubation in the solutions containing the DNAs, $(i_0 - i)/i_0$ (shown in Fig. 2A), similarly to our previous reports(Aoki et al., 2010a, b). The normalized current change of $(i_0 - i)/i_0$ was depicted on a pseudocolor scale ranging from green (low) to red (high) (Fig. 2C–D).

3. Results and discussion

3.1. 384-Ch electrode array chip

The fabricated electrode array chip was electrochemically investigated using $[Fe(CN)_6]^{4-}$ as an electroactive marker, in a similar manner to that reported in previous papers (Aoki et al., 2010a, b). Cyclic voltammograms (CVs) of the $[Fe(CN)_6]^{4-}$ marker for 384 electrodes on the chip were investigated. While these 384 electrodes show reversible or quasi-reversible responses (i.e., the differences between oxidative and reductive peak current potentials (ΔE_p) of the observed

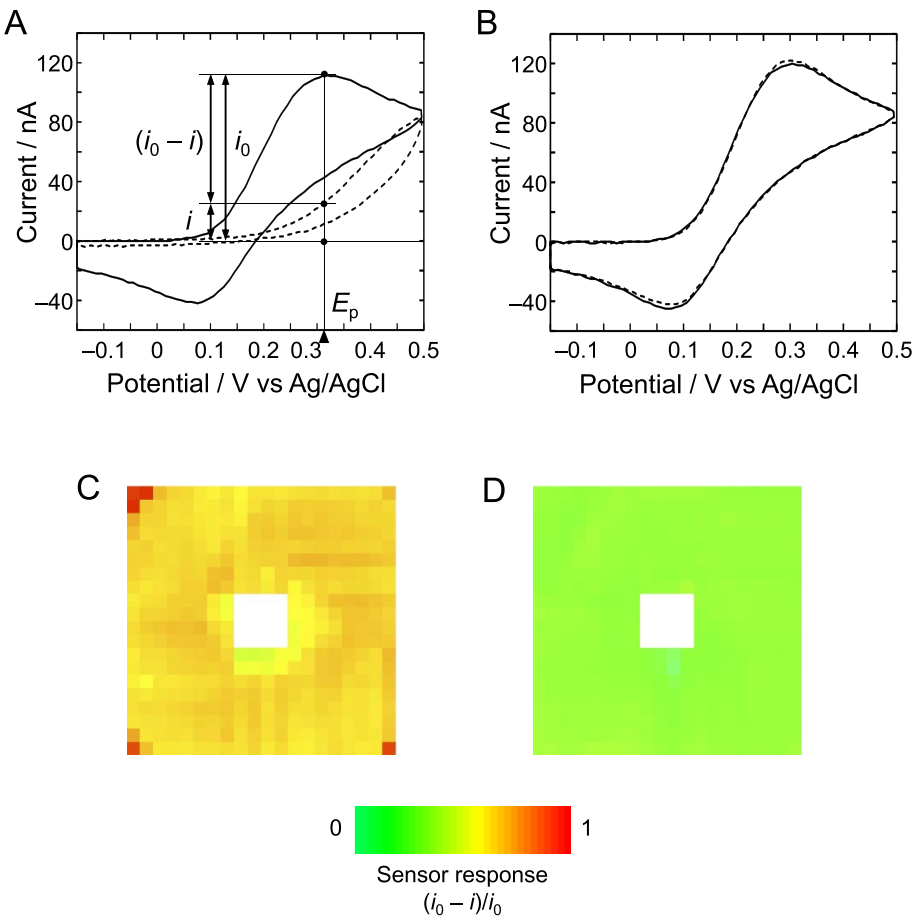

Fig. 2. CVs of 1 mM $[Fe(CN)_6]^{4-}$ marker for typical sensors in the fabricated electrode array chip after modification with PNA_1 (solid line in A and B) and incubation in 100-μM solutions of target (DNA_1, dashed line in A) and mismatch (DNA_2, dashed line in B) DNAs. The 384 sensor responses for PNA_1 sensors incubated in solutions of target (DNA_1, C) and mismatch (DNA_2, D). Sensor responses are depicted on a pseudocolor scale ranging from green (low) to red (high).

CVs were around 60–100 mV), a slight trend was observed for the electrodes in the more central areas to show larger ΔE_p values and the electrodes in more peripheral areas to show smaller ΔE_p values (Fig. S1). This trend is also observed when using other electrode array chips, even after changing the order of electrodes for recording CVs. This observed trend of the inconsistency of plasma treatment may be due to the arrangement of the conductive areas on the chip, which might in turn affect exposure conditions to plasma irradiation(Abuzairi et al., 2016; Zaplotnik et al., 2015). We believe that this inconsistency of plasma treatment was unlikely to have had a significant influence on the following experiments, and that it is more important to focus on relative signal changes before and after the target recognition, normalized by subtracting the baseline from the observed signal.

3.2. Probe PNA-based sensor array chip

After electrochemical investigation of the fabricated electrode array chip, PNA_1 and HHT were immobilized on the plasma-treated electrode array chip to prepare a sensor array chip. CVs of $[Fe(CN)_6]^{4-}$ marker for the 384 sensors prepared on the chip were observed to be quasi-reversible, as shown in Fig. 2A (solid line) for a typical sensor. Next, a 100-μL aliquot of aqueous solution containing 100 μM target DNA_1 with a complementary sequence to probe PNA_e3 was dropped onto the sensor array chip. The chip was covered with a cover glass and kept in a humid chamber for 40 min at 25 °C during the incubation process. After incubation, the CVs of the $[Fe(CN)_6]^{4-}$ marker showed an irreversible redox reaction on the part of the marker, shown in Fig. 2A (dashed line). This is because the hybridization of target DNA_1 with probe PNA_1 caused a negative surface charge on the electrode and, concomitantly, induced electrostatic repulsion between the negatively charged marker and the negatively charged surface, inhibiting the redox reaction of the marker at the electrode surface. This result is consistent with those in previous studies(Aoki et al., 2000; Aoki and Tao, 2005). We also incubated another sensor array chip for probe PNA_1 in a 100-μL aliquot of aqueous solution containing 100 μM mismatch DNA_2 with an unrelated sequence, and made electrochemical measurements in the same manner. In this case, however, the observed CVs showed almost the same CVs as before incubation, shown in Fig. 2B (dashed line). This result indicates that the sensors prepared on the chip have the capability to distinguish oligonucleotides sequence-specifically. The sensor has potential to be repeatedly used by regenerating the device with the incubation in an aqueous solution of urea, as we previously reported(Aoki and Tao, 2007). But, in this study, we focused on the single use of the chips as “one-time” disposable devices to prevent false positives in environmental and biomedical applications.

Here, to be able to evaluate all the 384 sensor responses for the sensor array chip, the sensor response to the DNAs is expressed as the ratio of the current decrease $(i_0 - i)$ to peak current (i_0) at the peak potential (E_p) in the CVs measured before incubation in the solutions containing the DNAs, $(i_0 - i)/i_0$ (See Material and methods and Fig. 2A). The normalized current change of $(i_0 - i)/i_0$ was depicted using a pseudocolor scale ranging from green (low) to red (high). The results are shown in Fig. 2C–D, in which the values of the normalized current changes are shown as 0.504 ± 0.0581 and 0.000861 ± 0.0596 for the target (C) and mismatch (D), respectively. Virtually all of the sensors showed sequence-specific responses, while some sensors in peripheral areas showed rather stronger responses and sensors in central areas showed somewhat weaker responses, as shown in Fig. 2C. Although this inconsistent response trend is still noticeable, similar to that shown in Section 3.1, the expression of sensor responses in the normalization of current change in CVs outweighs this trend.

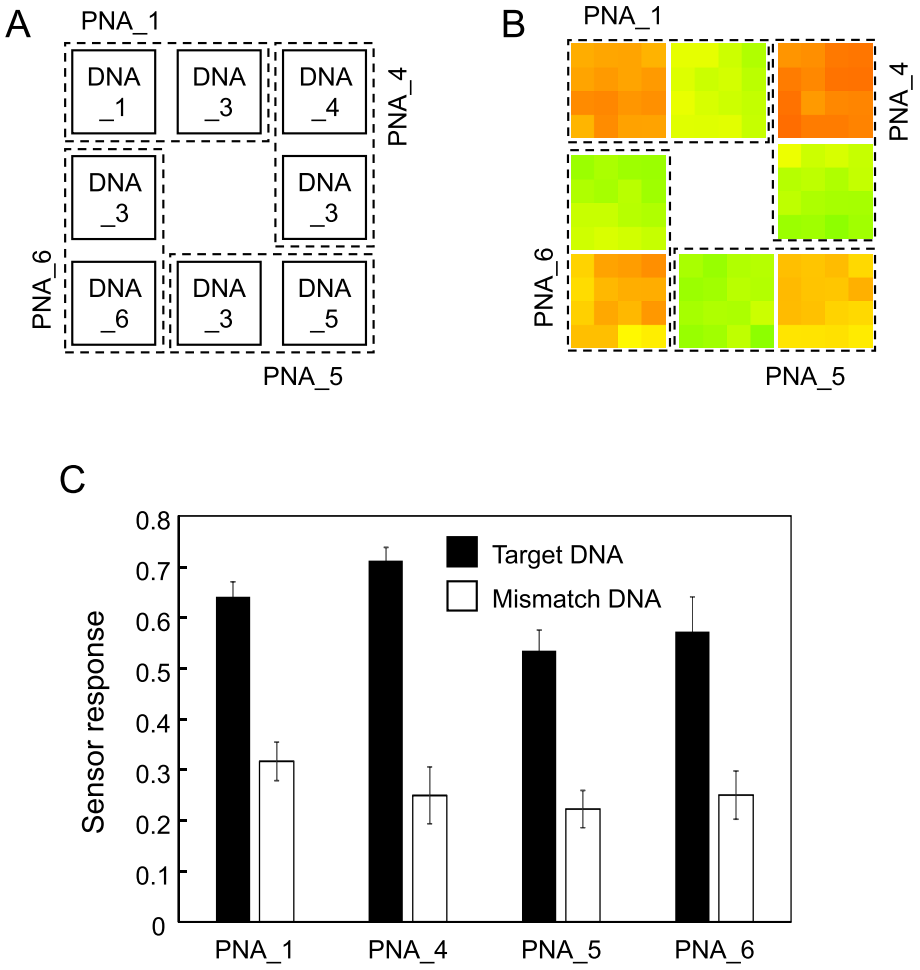

Fig. 3. Eight-array blocks modified with corresponding biomedically-significant probe PNAs, incubated in solutions of target and mismatch DNAs (A) to record the sensor responses (B) in the same manner as those in Fig. 2. The sensor responses are summarized in (C).

3.3. Simultaneous detection of environmentally- and biomedically-relevant oligonucleotides

Multiple oligonucleotide detection is the key to utilization of oligonucleotide detection techniques as diagnosis tools in the environmental and biomedical fields. For example, biological evaluation of chemical substances requires the simultaneous detection of tens or hundreds of oligonucleotide sequences(McCormick and Nuwaysir, 2005). This prompted us to use 384-ch sensor array chips for the simultaneous detection of oligonucleotides with environmentally- and biomedically-relevant sequences.

A hydrophobic adhesive film with eight open windows (Fig. 1D) was prepared and used for the modification of the electrode array chip with multiple probe PNAs. This film has eight windows that independently separate the electrode area on the chip during modification and incubation. Each window covers a 4 × 4 electrode array block (Fig. 3A). The electrodes for the eight blocks were modified with four kinds of probe PNAs (PNA_1, PNA_4, PNA_5, and PNA_6) targeting environmentally- and biologically-relevant sequences. After the modification process, these eight blocks were subjected to incubation in 10-μL aliquots of aqueous solutions containing 100 μM of the target (DNA_1, DNA_4, DNA_5, and DNA_6) or mismatch (DNA_3) oligonucleotides. Fig. 3B shows the sensor responses. Among these four probe PNAs, targets with complementary sequences to those of the probes showed higher responses, while mismatches with non-complementary sequences showed lower responses. Our results are summarized in Fig. 3C. The error bars show standard deviations for all the available sensor responses, clearly showing sequence-specific target recognition. Here, the four probe PNAs used in Fig. 3B showed similar responses to the corresponding target and mismatch DNAs. This is probably because of similar association constants for probe/target pairs. This result is supported by several empirical equations, as we mentioned in a previous report.(Aoki and Tao, 2005). Ratilainen et al., (2000) studied the relationship between the length and the binding thermodynamics using numerous probe PNA/target DNA pairs and found that the association constants for *N*-mer PNA/DNAs at 25 °C follow the below equation.

$$K_{25\_Ratilainen} = (14 \pm 1)^N \quad (1)$$

The length of the probes used is 20 mer. The estimated $K_{25\_Ratilainen}$ value is derived as $8.37 \times 10^{22}\,M^{-1}$. The observed result is also supported by another model, reported by Giesen et al., (1998), which takes into account not only the length but also the base pair sequence. Giesen et al. developed a model of melting temperature (T_m) as a good measure of the stability of a PNA/DNA duplex, employing the nearest-neighbor approach,

$$T_{m\_Giesen} = 20.79 + 0.83T_{m\_DNA/DNA} - 26.13f_{pyr} + 0.44l_{PNA} \quad (2)$$

where $T_{m\_DNA/DNA}$ is the T_m calculated using the nearest-neighbor model for the corresponding DNA/DNA duplex, applying values of change in enthalpy, $-\Delta H^\circ$, and change in entropy, $-\Delta S^\circ$, as described by SantaLucia et al., (1996) f_{pyr} is the fractional pyrimidine content in the PNA strands, and l_{PNA} is the length of the PNA sequence. The estimated T_{m_Giesen} values are 74.7, 77.3, 71.7, and 78.4 for PNA_1, PNA_4, PNA_5, and PNA_6, respectively, showing the probe/target pairs to be

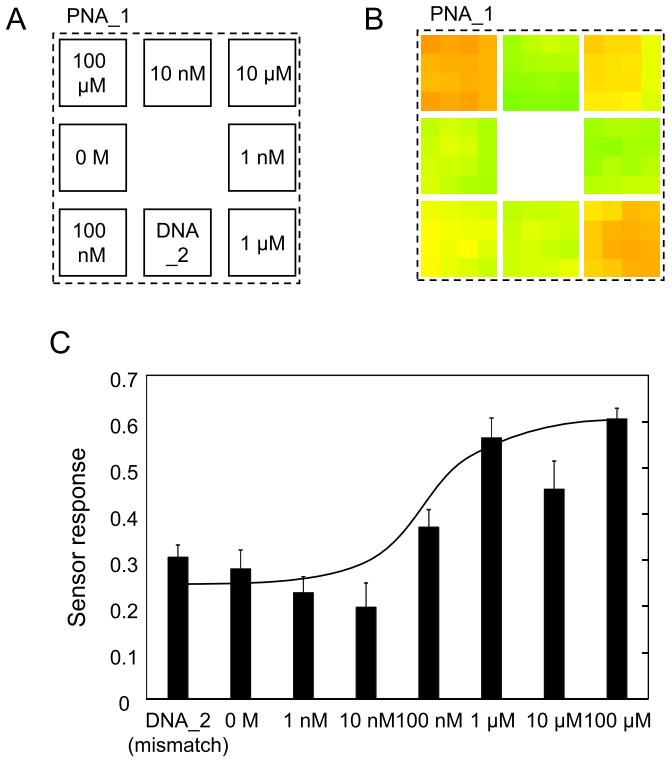

Fig. 4. Eight-array blocks modified with PNA_1, incubated in solutions of 100 μM of mismatch and 0 M, 1 nM, 10 nM, 100 nM, 1 μM, 10 μM, and 100 μM of target DNAs (A) to record the sensor responses (B) in the same manner as those in Fig. 2. The sensor responses are summarized in (C).

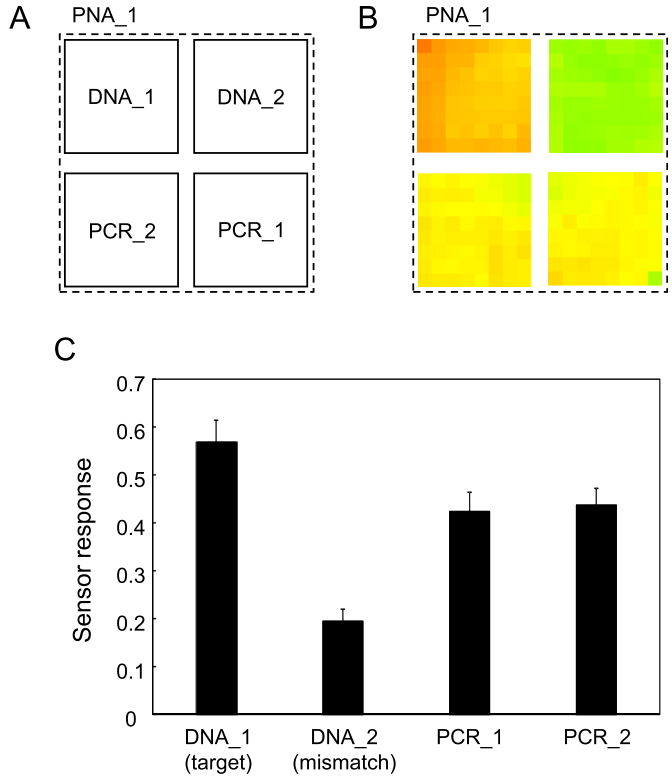

Fig. 5. Four-array blocks modified with PNA_1, incubated in 50-μM solutions of the target DNA_1 and mismatch DNA_2, 150 nM of PCR products of PCR_1 and PCR_2 (A) to record the sensor responses (B) in the same manner as those in Fig. 2. The sensor responses are summarized in (C).

similarly stable.

From these results, we concluded that the sensor array chips recognize environmentally- and biomedically-relevant targets.

3.4. Concentration-dependence of sensor responses

To investigate the limitations of the sensor array chips, we demonstrated the dependence of sensor responses on the target concentrations on a single chip. The electrodes were modified with the probe PNA_1 and the eight probe-modified blocks were then incubated in 10-μL aliquots of aqueous solutions containing 100 μM, 10 μM, 1 μM, 100 nM, 10 nM, 1 nM, and 0 M of the target DNA_1 and 100 μM of the mismatch DNA_2. To confirm that the solutions did not intermingle by crossing the hydrophobic barrier on the adhesive film, we put solutions next to others with a 1000-fold difference in the target concentrations (Fig. 4A). Sensor responses are shown in Fig. 4B. Fig. 4C, summarizing the results in Fig. 4B. They demonstrate a large change in sensor response in the range from 10 nM to 1 μM. The linear regression provided the relationship of [Sensor response] = 0.183 × log[DNA] + 1.66 with the R^2 value of 0.999, showing the linearity of the response in this range. Detailed investigations revealed a detection limit of 7.33×10^{-8} M (S/N = 3.0, where the standard deviation at 10 nM of 0.0529 was used as a noise.) and the relative standard deviation of the sensor responses (n = 16 at 1 μM of target DNA_1) proved to be < 10%. This value is one thousand-fold the detection limit of 7.50×10^{-11} M obtained in the previous research using gold disk electrodes, based on the same probe/target pair and the same working principle(Aoki and Tao, 2005). The reason for the observed higher detection limit is not clear, but we assume that it may be for reasons related to both the chips themselves (contaminant residues not removed from the surface and the resultant difference in the surface density of probe PNAs between the microelectrodes) and the adhesive films (leakage of some contaminants from the adhesive films or mixing of the solutions with others via the films). Further optimization of the fabrication of the chips or the adhesive films might be needed to improve the detection limit. In contrast, sensor response to 100 μM of the non-complementary DNA_2 solution was similar to that for the 0 M solutions. We therefore concluded that the sensor responses were sequence-specific and dependent on the concentration of the target. In this study, we investigated the pair of PNA_1/DNA_1 to induce the detection limit, but it can be easily applied to other pairs listed in Table 1 to induce the detection limits on the single chip.

3.5. PCR-amplified samples

For application to real samples, we demonstrated the detection of target DNAs based on oligonucleotide samples amplified by PCR. The electrodes on the chip were modified with PNA_1, and the prepared sensors were separately incubated in aqueous solutions containing different oligonucleotides, as depicted in Fig. 5A. In this study, a hydrophobic adhesive film with four windows open to 8 × 8 electrode array blocks was used to obtain sensor responses to four kinds of oligonucleotides. For measurement, we used 12.5-μL aliquots of aqueous solutions containing 50 μM of target DNA_1, 50 μM of mismatch DNA_2, 150 nM of PCR_1, and 150 nM of PCR_2 for PNA_1 sensors. PCR_1 or PCR_2 of 70-mer length were produced by amplifying a 100-mer template using Primers PCR_11 and PCR_12 or PCR_21 and PCR_22, respectively, to prepare the sample solutions with concentrations of 150 nM after the gel-based standard purification described in Material and methods. Sensor responses are shown in Fig. 5B and are summarized in Fig. 5C. Target DNA_1 showed sequence-specific responses to mismatch DNA_2. PCR_1 and PCR_2 also clearly showed responses.

Interestingly, PCR_1 and PCR_2 showed similar responses despite their different positions captured by, or complementary to, probe PNA_1 in the sequences. The capture position of PCR_1 is in the center

of the sequence and, in hybridization, extends not only an overhanging single-stranded DNA tail at the 5′ terminal to the bulk solution but also a tail at the 3′ terminal to the sensor surface. In contrast, the capture position of PCR_2 is at the end of the 5′ terminal and, in hybridization, extends a tail only at the 3′ terminal to the bulk solution. We expected, therefore, that hybridization of PCR_1 to PNA_1 would be sterically hindered and that the observed sensor response would therefore be smaller than that for PCR_2. It is generally known that the lengths of linkers tethering probes to the surface and the lengths of overhanging tails of target oligonucleotides extending both to the surface and to the bulk solution can affect the efficiency of hybridization at the surface, according to previous reports based on theoretical analysis(Peytavi et al., 2005) and optical experiments(Halperin et al., 2006). It is not clear why PCR_1 and PCR_2 showed similar responses, but it could have resulted from the long overhanging tails of these oligonucleotides affecting the hybridization efficiency.

4. Conclusion

We investigated the detection of multiple environmentally- and biomedically-relevant RNA biomarker sequences on a single newly-fabricated 384-ch sensor array chip aiming at practical application. The chips showed sequence-specific sensor responses upon hybridization with targets but far less so with mismatches. The dependence of sensor responses on target concentrations was observed, with a detection limit of 7.33×10^{-8} M (S/N = 3.0) and a relative standard deviation of < 10% (n = 16 at 1 μM of target DNA_1). As more realistic samples, PCR-amplified oligonucleotide samples were applied to the chips and showed sequence-specific responses, revealing that the fabricated sensor array chips have potential for use with PCR samples.

Recent innovations and the development of novel sequencers are opening the way to the use of nanotechnology-based miniaturized sequencers in environmental and healthcare management (Oxford Nanopore Technologies, 2018; Pac Bio, 2018). However, we believe that sensor array chips focusing on known oligonucleotides will play an important role in biomarker screening, which will need simple, rapid, and “one-time” disposable devices to prevent false positives in environmental and biomedical applications, in contrast to the current complicated and expensive chips. Our sensor array chips that use glass coated with gold thin films are simple and fabricated from inexpensive and readily available materials(Aoki, 2015; Zhang et al., 2017). This technique is likely to make environmental and biomedical diagnoses simpler and easier to carry out.

For healthcare applications to clinical diagnosis, considerable efforts have been made to find RNA biomarkers, including miRNAs, as cancer biomarkers of the type employed in this study(Angelini and Emanueli, 2015; Montani et al., 2015; Wang et al., 2016). For environmental applications to evaluate chemical toxicity, research in the new field of toxicogenomics has led to organized public projects to find RNA biomarkers including mRNAs as estrogen-responsive genes of the type employed here, and to publish them in databases(Borlak, 2005; Igarashi et al., 2015; Minami et al., 2014; Waters and Fostel, 2004). We also have been searching for RNA biomarkers that are more sensitive to chemical stress, since both sensor array development and biomarker searching are crucially important to develop feasible screening techniques(Tani et al., 2017). We believe that we will be able report other novel sensor array chips based on our newly-identified RNA biomarkers in the near future.

Declaration of competing interests

The authors declare that they have no known competing financial interests or personal relationships that could have appeared to influence the work reported in this paper.

The authors declare the following financial interests/personal relationships which may be considered as potential competing interests.

CRediT authorship contribution statement

Hiroshi Aoki: Conceptualization, Methodology, Data curation, Formal analysis, Writing - original draft, Writing - review & editing. **Masaki Torimura:** Conceptualization, Writing - review & editing. **Tetsuya Nakazato:** Conceptualization, Writing - review & editing.

Acknowledgements

This work was partially supported by JSPS KAKENHI Grant Number JP15K0189 (awarded to HA).

Appendix A. Supplementary data

Supplementary data to this article can be found online at https://doi.org/10.1016/j.bios.2019.04.047.

References

Abuzairi, T., Okada, M., Bhattacharjee, S., Nagatsu, M., 2016. Surface conductivity dependent dynamic behaviour of an ultrafine atmospheric pressure plasma jet for microscale surface processing. Appl. Surf. Sci. 390, 489–496.
Alexander-Dann, B., Pruteanu, L.L., Oerton, E., Sharma, N., Berindan-Neagoe, I., Módos, D., Bender, A., 2018. Developments in toxicogenomics: understanding and predicting compound-induced toxicity from gene expression data. Mol. Omics 14 (4), 218–236.
Angelini, T.G., Emanueli, C., 2015. MicroRNAs as clinical biomarkers? Front. Genet. 6 (240), 240.
Aoki, H., 2012. Development of novel gene detection methods and its application to rapid environmental diagnostic techniques. Bunseki Kagaku 61, 763–776.
Aoki, H., 2015. Electrochemical label-free nucleotide sensors. Chem. Asian J. 10, 2560–2573.
Aoki, H., Bühlmann, P., Umezawa, Y., 2000. Electrochemical detection of a one-base mismatch in an oligonucleotide using ion-channel sensors with self-assembled PNA monolayers. Electroanalysis 12 (16), 1272–1276.
Aoki, H., Kitajima, A., Tao, H., 2010a. Electrochemical gene sensor arrays prepared using non-contact nanoliter array spotting of gene probes. Anal. Sci. 26, 367–370.
Aoki, H., Kitajima, A., Tao, H., 2010b. Electrochemical sensor array chips for multiple gene detection. Sensor. Mater. 22 (7), 327–336.
Aoki, H., Tao, H., 2005. Gene sensors based on peptide nucleic acid (PNA) probes: relationship between sensor sensitivity and probe/target duplex stability. Analyst 130 (11), 1478–1482.
Aoki, H., Tao, H., 2007. Label- and marker-free gene detection based on hybridization-induced conformational flexibility changes in a ferrocene-PNA conjugate probe. Analyst 132 (8), 784–791.
Bard, A.J., Faulkner, L.R., 2001. Electrochemical Methods: Fundamentals and Applications, second ed. John Wiley & Sons, New York.
Bonci, D., Coppola, V., Patrizii, M., Addario, A., Cannistraci, A., Francescangeli, F., Pecci, R., Muto, G., Collura, D., Bedini, R., Zeuner, A., Valtieri, M., Sentinelli, S., Benassi, M.S., Gallucci, M., Carlini, P., Piccolo, S., De Maria, R., 2016. A microRNA code for prostate cancer metastasis. Oncogene 35 (9), 1180–1192.
Borlak, J., 2005. Handbook of Toxicogenomics. Wiley-VCH, New York.
Campana, O., Wlodkowic, D., 2018. Ecotoxicology goes on a chip: embracing miniaturized bioanalysis in aquatic risk assessment. Environ. Sci. Technol. 52 (3), 932–946.
CAS Registry, visited in April 25, 2018. CAS REGISTRY - the Gold Standard for Chemical Substance Information. http://support.cas.org/content/chemical-substances.
Fiammengo, R., 2017. Can nanotechnology improve cancer diagnosis through miRNA detection? Biomark. Med. 11 (1), 69–86.
Giesen, U., Kleider, W., Berding, C., Geiger, A., Ørum, H., Nielsen, P.E., 1998. A formula for thermal stability (Tm) prediction of PNA/DNA duplexes. Nucleic Acids Res. 26 (21), 5004–5006.
Halperin, A., Buhot, A., Zhulina, E.B., 2006. Hybridization at a surface: the role of spacers in DNA microarrays. Langmuir 22 (26), 11290–11304.
Huang, Y.C., 2013. The role of in vitro gene expression profiling in particulate matter health research. J. Toxicol. Environ. Health B 16 (6), 381–394.
Igarashi, Y., Nakatsu, N., Yamashita, T., Ono, A., Ohno, Y., Urushidani, T., Yamada, H., 2015. Open TG-GATEs: a large-scale toxicogenomics database. Nucleic Acids Res. 43 (Database issue), D921–D927.
Kim, S.-H., Lee, S.-Y., Lee, Y.-M., Lee, Y.-K., 2015. MicroRNAs as biomarkers for dental diseases. Singapore Dent. J. 36, 18–22.
Kreth, S., Hübner, M., Hinske, L.C., 2018. MicroRNAs as clinical biomarkers and therapeutic tools in perioperative medicine. Anesth. Analg. 126 (2), 670–681.
Lucarelli, F., Tombelli, S., Minunni, M., Marrazza, G., Mascini, M., 2008. Electrochemical and piezoelectric DNA biosensors for hybridisation detection. Anal. Chim. Acta 609 (2), 139–159.
McCormick, M., Nuwaysir, E.F., 2005. Toxicogenomics applications of open-platform high density DNA microarrays. In: Borlak, J. (Ed.), Handbook of Toxicogenomics. Wiley-VCH, New York, pp. 83–95.

Minami, K., Uehara, T., Morikawa, Y., Omura, K., Kanki, M., Horinouchi, A., Ono, A., Yamada, H., Ohno, Y., Urushidani, T., 2014. miRNA expression atlas in male rat. Sci. Data 27, 140005.
Montani, F., Marzi, M.J., Dezi, F., Dama, E., Carletti, R.M., Bonizzi, G., Bertolotti, R., Bellomi, M., Rampinelli, C., Maisonneuve, P., Spaggiari, L., Veronesi, G., Nicassio, F., Di Fiore, P.P., Bianchi, F., 2015. miR-test: a blood test for lung cancer early detection. J. Natl. Cancer Inst. 107 (6) djv063.
National Center for Biotechnology Information, visited in April 25, 2018. https://www.ncbi.nlm.nih.gov/.
Oxford Nanopore Technologies, visited in April 25, 2018. https://nanoporetech.com/.
Pac Bio, visited in April 25, 2018. https://www.pacb.com/.
Paleček, E., Bartošík, M., 2012. Electrochemistry of nucleic acids. Chem. Rev. 112 (6), 3427–3481.
Peytavi, R., Tang, L., Raymond, F.R., Boissinot, K., Bissonnette, L., Boissinot, M., Picard, F.J., Huletsky, A., Ouellette, M., Bergeron, M.G., 2005. Correlation between microarray DNA hybridization efficiency and the position of short capture probe on the target nucleic acid. Biotechniques 39 (1), 89–96.
Promega, visited in April 25, 2018. https://www.promega.com/resources/protocols/technical-bulletins/101/wizard-sv-gel-and-pcr-cleanup-system-protocol/?cs=y.
Ratilainen, T., Holmén, A., Tuite, E., Nielsen, P.E., Nordén, B., 2000. Thermodynamics of sequence-specific binding of PNA to DNA. Biochem 39, 7781–7791.
Sadik, O.A., Aluoch, A.O., Zhou, A., 2009. Status of biomolecular recognition using electrochemical techniques. Biosens. Bioelecton. 24 (9), 2749–2765.
SantaLucia Jr., J., Allawi, H.T., Seneviratne, P.A., 1996. Improved nearest-neighbor parameters for predicting DNA duplex stability. Biochem 35, 3555–3562.
Sassolas, A., Leca-Bouvier, B.D., Blum, L.J., 2008. DNA biosensors and microarrays. Chem. Rev. 108 (1), 109–139.
Takara Bio, visited in April 25, 2018. http://catalog.takara-bio.co.jp/product/basic_info.php?unitid=U100003782.
Tani, H., Takeshita, J., Aoki, H., Nakamura, K., Abe, R., Toyoda, A., Endo, Y., Miyamoto, S., Gamo, M., Sato, H., Torimura, M., 2017. Identification of RNA biomarkers for chemical safety screening in mouse embryonic stem cells using RNA deep sequencing analysis. PLoS One 12 (7), e0182032.
Teles, F.R.R., Fonseca, L.R., 2008. Trends in DNA biosensors. Talanta 77 (2), 606–623.
Wagner, E.D., Plewa, M.J., 2017. CHO cell cytotoxicity and genotoxicity analyses of disinfection by-products: an updated review. J. Environ. Sci. 58, 64–76.
Wang, J., 2005. Electrochemical nucleic acid biosensors. In: Paleček, E., Scheller, F., Wang, J. (Eds.), Electrochemistry of Nucleic Acids and Proteins: towards Electrochemical Sensors for Genomics and Proteomics. Elsevier, pp. 175–194.
Wang, J., 2006. Electrochemical biosensors: towards point-of-care cancer diagnostics. Biosens. Bioelecton. 21 (10), 1887–1892.
Wang, J., Chen, J., Sen, S., 2016. MicroRNA as biomarkers and diagnostics. J. Cell. Physiol. 231 (1), 25–30.
Waters, M.D., Fostel, J.M., 2004. Toxicogenomics and systems toxicology: aims and prospects. Nat. Rev. Genet. 5 (12), 936–948.
Zaplotnik, R., Bišćan, M., Kregar, Z., Cvelbar, U., Mozetič, M., Milošević, S., 2015. Influence of a sample surface on single electrode atmospheric plasma jet parameters. Spectrochim. Acta B 103–104, 124–130.
Zhang, H., Oellers, T., Feng, W., Abdulazim, T., Saw, E.N., Ludwig, A., Levkin, P.A., Plumere, N., 2017. High-density droplet microarray of individually addressable electrochemical cells. Anal. Chem. 89 (11), 5832–5839.